Joint Multi-view Feature Network for Automatic Diagnosis of Pneumonia with CT Images

Hao Cui, Fujiao Ju*, and Jianqiang Li

Faculty of Information Technology, Beijing University of Technology, Beijing 100124, China
jfj2017@bjut.edu.cn

Abstract. Automated recognition of pneumonia from chest CT plays an important role in the subsequent clinical treatment for patients. While a few pioneering works only focus on several random slices from chest CT image, thus they have ignored the anatomical dependency information of local lesions. Considering it, this paper explores a novel automatic classification method for pneumonia detection based on fusing regional and global information, which not only improves detection performance, but also provides explainable diagnostic basis for radiologists. Firstly, identifying the interested local region by a lesion detection module, then we extracts the correlation relationship between local regions through a graph attention module. The image-level classification results can be acquired by fusing the information of global and local region. To realize the detection of full CT sequence, a person-level classifier is designed in the proposed model. In the experiment, we collected 781 chest CT sequences in total corresponding to 274 cases of viral pneumonia patients, 285 cases of bacterial pneumonia patients and 222 cases of healthy people. The experimental results show that our model achieves the accuracy of 95.5%, with 95.6% precision and 0.991 AUC. The recall and F1 score are 95.8% and 95.7% respectively, which outperformed previous works. Therefore, our method can be regarded as an efficient assisted tool in the diagnose of pneumonia.

Keywords: Pneumonia diagnosis, Chest CT sequence, Graph network, Multi-view feature fusion

1 Introduction

Pneumonia is one of the greatest threats for human health, which can spread world-wide especially for viral pneumonia with strong transmissibility. The clinical practice shows that the main factors causing pneumonia are virus, bacteria, fungi and mycoplasma [1]. Due to the distinction of etiology and clinical manifestations of different types of pneumonia [2], the treatment measures for patients should be formulated according to their image findings. At present, the diagnosis of different types of pneumonia can be preliminarily determined by Chest X-Ray(CXR). However, the resolution of CXR is too low that it is difficult to

detect the lesions, resulting in misdiagnosis [3]. As chest Computed Tomography(CT) scan provides more detailed cross-sections of the organ, it is regarded as the most effective and commonly used imaging technique for diagnosing many diseases [4], [5]. Moreover, the chest CT scans of different pneumonia patients show different characteristics. For bacterial pneumonia patients, the chest CT scans mainly show pulmonary parenchymal involvement, lung consolidation and central lobular nodules or tree buds sign, while the chest CT infected by virus mainly shows ground glass opacity, grid opacity and paving stone sign [6]. Therefore, radiologists often make preliminary etiological judgments based on the patient's CT scans. In recent years, pneumonia patients have gradually increased, accompanied by a significant increase in the number of chest CT scans, which leads to a serious shortage of experienced radiologists [7]. Due to the complexity of lung structure, the lesions of different pneumonia are difficult to distinguish, thus it becomes a serious challenge for doctors to diagnose quickly and accurately, especially when respiratory infectious breakout in a large scale. Therefore, it is extremely important to establish a automatic system to assist the clinical practice in speeding up screening and improving the diagnose accuracy.

This study is based on the collected chest CT scans containing viral pneumonia, bacterial pneumonia patients and healthy person in the Beijing area. In this paper, we explore a joint multi-view feature network (JMFNet) for automatic diagnosis of pneumonia with CT images. Firstly, extracting the global features of CT images by a backbone, then we find the interested local regions by adding a object detection branch on backbone. Next, a graph attention module is used to extract the correlation information between local regions. By fusing the information of global slice and local region, we can obtain the classification results of each slice. Finally, for a full chest CT sequence, we design a person-level prediction mechanism to simulate the diagnostic process in clinical operations.

The main contributions of this paper are summarized as follows:

- To simulate the radiologist's diagnosis process, we construct a automatic pneumonia diagnosis system based on full CT sequence prediction, so as to avoid missed diagnosis or misdiagnosis;
- To focus on the key regions, we extract the interested lesions by a object detection branch and mine the relative position dependencies between lesion regions;
- To improve the accuracy of the automatic diagnosis system, we fuse the multi-view information from global and local region to construct recognition model and then provide interpretable analysis to assist doctor diagnosis.

2 Related Work

In clinical practice, radiologists usually observe CXR or CT scans to realize the diagnose of pneumonia [4]. To establish automatic diagnose system, the researchers try to explore machine learning algorithms, which can be mainly divided into two categories, traditional pattern recognition algorithms and deep

learning algorithms. In general, the traditional algorithms manually extract features and then construct classifier [8]. In [9], Jin C et al. use the public CXR dataset for feature selection, then compare the prediction results of decision tree, random forest and support vector machine models. Cheng Jin et al. [10] extract 12 characterizing features of CT slices and test that there is a significant difference between community acquired pneumonia (CAP) and COVID-19 by constructing the lasso regression model. However, the feature extractions based on pattern recognition algorithms mainly depend on the experience of experts and feature transformation, which lack abstract hidden information and result in limitations in performance improvement. As Convolutional Neural Networks (CNN) [11] have been successfully applied to the medical imaging, some researchers have attempted to combine traditional pattern recognition algorithms with deep learning to detect lung disease through CT scan or CXR. In [12], the authors propose CheXNet to extract CXR features by deep pre-training model and manual techniques. The most important features can be selected by combining principal component analysis (PCA) and recursive feature elimination (RFE). The final comparison shows that XGBoost classifier has the best performance.

Due to the excellent feature extraction ability of deep learning, researchers have intend to utilize deep learning algorithms to build lung disease diagnose models. Many works regard CT images classification as a coarse-grained classification task, and randomly select CT slices as input. For example, Shouliang Qi et al. [13] pick ten CT slices from a patient's CT sequence for feature extraction. Each slice is processed by ResNet50 [14] for feature extraction so as to obtain the prediction of each slice. The final prediction of a patient is generated by aggregating slice predictions. In general, the slices with lesions are unknown, thus randomly selecting slices may result in misdiagnosis, which is also inconsistent with the diagnose habits of radiologists. In addition, the most of the existing methods realize image-level prediction only using global features. The lesions in CT slices are easily confused, which lead to the low variance between different types of pneumonia. Therefore, subtle lesions containing the correlation between lesion areas are also important and critical. In [15], Ying Song et al. extract the main region of lung and design a details relation extraction neural network to obtain the image predictions. The person diagnosis are achieved by aggregating the image predictions.

Different pneumonia have different lesion distribution in the lung window. For viral pneumonia, lesions are distributed in the subpleura and lesions of bacterial pneumonia are distributed in the lung parenchyma. As graph neural networks (GNN) [16] performs well in acquiring the correlation between target nodes. Several studies have begun to utilize GNN to extract correlation information in medical image anlysis. In [17], the authors attempt to construct the graph by calculating the Euclidean distance between the extracted features vectors to predict the viral pneumonia via CT. To utilize the similarity and co-occurrence between lesions, in this study, we segment the interested local region and construct the graph attention network [18] based on lesions. By analyzing the joint multi-view

features, we design a automatic diagnosis of pneumonia with CT images. The specific model is introduced in the next section.

3 Method

3.1 Data collection and processing

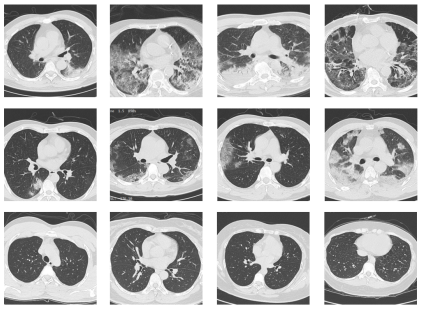

Fig. 1. The images in chest CT sequence of different pneumonia patients. The three rows show the lung images of bacterial, viral patient and healthy person from top to bottom, respectively.

This study is based on 781 plain chest CT sequences provided by Beijing Ditan Hospital and all patients are confirmed by clinical examination. The images of CT sequence are scanned at 5mm interval, and performed with a spiral scan after inspiratory breath hold. Each image contains detection time, detection specification and other parameters. In order to pay more attention to the information in lung window, we crop the original CT images to ensure that the contents of the lung window are preserved and the noise is removed. As a 3D CT sequence of one patient contains more then 300 images, we delete the images without lung parenchyma. Considering adjacent images are highly similar, we select 64 representative images with lesions to speed up the calculation [19]. Finally, the collected dataset includes 274 viral pneumonia patients with 16387 images, 285 bacterial pneumonia patients with 15848 images and 222 healthy person with 14208 images. Fig. 1 shows several CT images of different types of pneumonia patients.

3.2 Model architecture

This paper proposes an automatic pneumonia diagnosis system based on graph attention mechanism utilizing chest CT sequence. We firstly introduce the process of image-level pneumonia detection, which is based on fusing multi-view information of the interested regions and whole image. After that, the designed

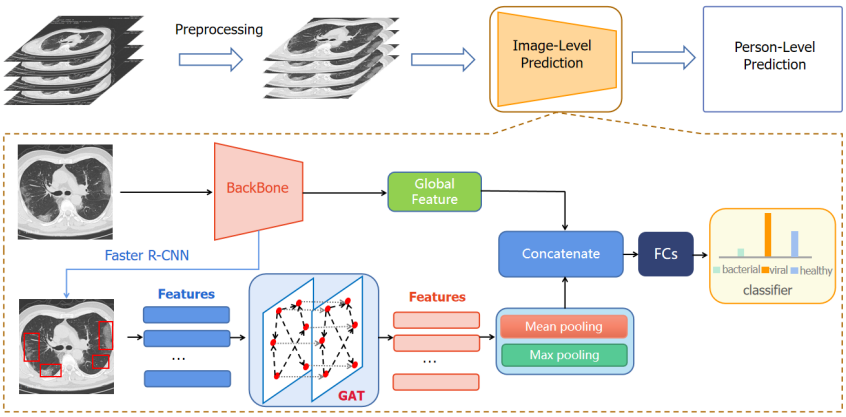

Fig. 2. The architecture of JMFNet. Extracting the global features of CT images and then a fast R-CNN branch is used to detect the top-k local lesion regions. Then the obtained local region features are fed to a graph attention neural network. Two pooling operations are performed on the aggregated k features, and they are combined with the global features and sent into the dense network for the final image-level classification. Finally, the person-level prediction is obtained based on all image classification results.

person-level classifier is introduced based on the image-level classification results. The model architecture is shown in Fig. 2.

In the proposed model, the collected CT images are preprocessed by converting dicom format to png images and removing boundary regions around the lungs. Then all images are input to the image-level prediction module. In this module, we extract the feature map and global features by a backbone network. The feature maps are then input to Faster R-CNN [20] to detect lesion regions. To explore the relationship between the anatomical regions in the CT image, we use a graph attention network (GAT) [16] to learn their dependencies. Finally, we combined the localized region features and global features to realize image-level prediction. Based on the image-level prediction results, we design a person-level classifier.

Defining a chest CT dataset as $X = \{x_1, x_2, ..., x_N\}$, x_i represents a patient CT slice. All the images are input to a backbone network to extract global features. To focus on local lesion information, a Faster R-CNN branch [20] is added on the backbone and we embed Feature Pyramid module (FPN) [21] in Faster R-CNN to detect lesions with different size. In this way, we obtain top k detection regions with the highest score as local information. As the detected interested regions have no uniform size, thus we need to normalize the size of regions to a unified value for the subsequent operations. In the experiments, the detected regions are resized to $112 * 112$. Finally, the features of the top k

anatomical regions in image x_i as H_i can be denoted as,

$$H_i = f(x_i) = \{h_1, h_2, ..., h_{k-1}, h_k\} \in \mathbb{R}^{k \times d}.$$

We take those k region features as the nodes of the graph to explores the correlation relationship. The new embedding expression h_i' can be updated as follows,

$$h_i' = \sigma\left(\sum_{j \in N_i} a_{ij} W h_j\right) \tag{1}$$

where $W \in \mathbb{R}^{d \times d}$ is the learned weight matrix, N_i represents the notes in the neighbor of node i and $\sigma(\cdot)$ denotes the nonlinear activation function. In addition, a_{ij} is the normalized importance weight coefficient of node j for node i, which can be calculated as follows:

$$a_{ij} = softmax_j(e_{ij}) = \frac{\exp(e_{ij})}{\sum_{k \in N_i} \exp(e_{ik})}$$

where

$$e_{ij} = LeakyReLU\left(a^T W h_i \parallel W h_j\right),$$

which represents the importance of the node j to node i and a is a weight vector.

By introducing the attention mechanism into the graph network, the correlation between different focal areas can be better integrated into the model. The neighbor nodes in (1) can be determined by similarity matrix S_{ij},

$$S_{ij} = \frac{h_i \cdot h_j}{\|h_i\| \, \|h_j\|} \tag{2}$$

We set a similarity threshold θ to judge whether the nodes are the first-order neighbors. If $S_{ij} > \theta$, node j is a neighbor of node i, otherwise node j does not belong to the neighbor of node i.

The obtained k region embeddings h' have been transferred to mean pooling and max pooling operation. Finally, we concatenated the global features and graph embeddings of local region to a 1-D vector and then sent them into a full connection layer and Softmax classifier. The loss function in the image-level prediction is computed by cross-entropy function,

$$\ell = -\sum_{c=1}^{C} \sum_{i=1}^{N} y_{ic} \log y_{ic}' \tag{3}$$

where C is the class number, y_{ic} and y_{ic}' are ground truth and predicted label, respectively.

3.3 The Person-level Classifier

In the image-level prediction, we not only obtain the prediction label of each training image, but also get the probability belonging to the corresponding label. By utilizing the image-level prediction results, we design the person-level prediction method, which contains two steps. The first step is the judgment for healthy person. If all the image-level prediction results of a full CT sequence are healthy, we can conclude that the person-level prediction of the test sample is health person. Otherwise, the test sample is from bacterial or viral pneumonia, which can be determined by the second step. In this step, deleting the slices with healthy prediction results, then we perform averaging operations on the remaining slices. Comparing the average distribution probability of bacterial and viral pneumonia, and finding out the largest value, then the test sample is divided into the label corresponding to the largest average value.

4 EXPERIMENT AND RESULTS

4.1 Implementation and Evaluation

For the requirement of hospital, we have designed two classification tasks: discriminating between viral and bacterial infected patients, and separating viral patients from bacterial patients and healthy person. In the experiments, we extract 4 or 6 interested lesion regions in each CT image and the five-fold validation is used to assess robustness and the performance of the model. In each fold, we randomly split the dataset according to the ratio of 6:2:2 for training, validation and testing.

For the initialization of the model, the learning rate is set to 0.0001 and Adam optimizer is selected to update the parameters. All the codes are implemented in Pytorch and performed on a server with Nvidia GeForce GTX 3090 GPUs. To assess the performance of the proposed model, the accuracy, precision, F1 score and recall are used as metrics to measure the evaluation of the classification results.

4.2 Experiment results and analysis

In this section, we have introduced the detailed description of binary and three-classification tasks.

Binary Classification Task For the classification of viral and bacterial pneumonia, we divide the dataset into three groups in the each fold: one group contains 164 viral and 171 bacterial pneumonia patients for training, the second group is for validation with 56 viral and 57 bacterial pneumonia patients, the last group contains 54 viral and 57 bacterial pneumonia patients for testing. We compared the results of different backbones consist of VGG-16 [22], GoogLeNet [23], DenseNet-121 [24], ResNet-50 [14] and ResNet-101 [14]. All the architectures are pre-trained on ImageNet for transfer learning.

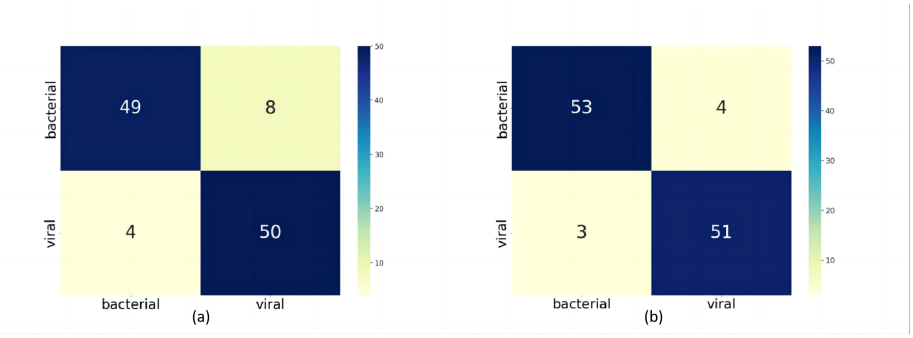

Fig. 3. Confusion matrix for binary classification tasks

Table.1 shows the results of different architectures. From the table we can see that the architecture ResNet-50 can achieve the highest classification accuracy of 86.5% and 88.4% for precision. For the recall and F1 score, the highest results are 87.3% and 86.5% acquired by DenseNet-121 and GoogLeNet, respectively. ResNet-50 have obtained 86.8% recall and 86.4% F1 score, which are just lower slightly than that of DenseNet-121. Thus, we choose ResNet-50 as the backbone of the proposed model for global feature extraction. In the pro-

Table 1. Comparison of different architectures

Method	Accuracy	Precision	Recall	F1 score
VGG-16	0.842	0.801	0.843	0.843
GoogLeNet	0.863	0.815	0.853	**0.865**
DenseNet-121	0.826	0.767	**0.873**	0.835
ResNet-50	**0.865**	**0.884**	0.868	0.864

posed model, we intend to extract the anatomical dependency information of local lesions by adding a Faster R-CNN branch on the backbone. To verify its superiority, we design ablation experiments and the results are listed in Table. 2. 'JMFNet w/o Local' means the proposed model without fusing local dependency information, which only extracts global features of slices for image-level classification. 'JMFNet w/o GAT' represents the model containing Faster R-CNN branch with global feature extraction module. 'JMFNet' lists the results of our proposed model, which has achieved obvious improvement. The ablation experiments have valid the effectiveness and superiority of fusing multi-view features. Except for ablation experiment, we also compare the classification results of other three methods, including DeCoVNet [25], AD3D-MIL [26] and DRENet [15]. Finally our model also obtain the higher results for all indicators. Fig. 3 (a) shows the confusion matrix of the proposed model. A total of 12 test samples are classified incorrectly. By analysis, we deduce that the reason for low accuracy is that

Table 2. Comparison of different methods for binary classification task

Method	Accuracy	Precision	Recall	F1 score
DeCoVNet	0.813	0.739	0.825	0.780
AD3D-MIL	0.848	0.762	**0.906**	0.828
DRENet	0.883	0.885	0.884	0.883
JMFNet w/o Local	0.865	0.884	0.868	0.864
JMFNet w/o GAT	0.875	0.890	0.882	0.884
JMFNet(our method)	**0.892**	**0.893**	0.893	**0.892**
JMFNet w/o healthy slices	**0.9369**	**0.9371**	**0.9367**	**0.9367**

the training dataset only contains the slices with viral and bacterial lesions in image-level prediction. However, the full CT sequence of a test sample consists of 200-230 slices, most of which may not contain lesions. Therefore, the slices without lesions would be identified as viral or bacterial infections, resulting in wrong results. Considering this, the healthy slices should be added to the training dataset in the image-level prediction even for the binary classification. The subsequent experiments have confirmed this point.

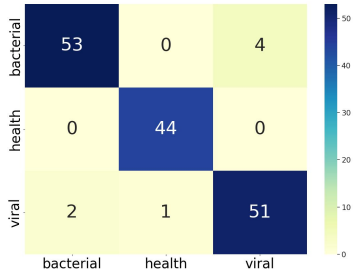

Fig. 4. Confusion matrix for three-classification task

Three-Classification Task According to the above analysis, we need to add healthy slice samples to the training set and train a three-classification model in the image-level prediction, even for the binary classification of virus and bacteria pneumonia. The training set contains 164 viral, 171 bacterial pneumonia patients and 134 healthy person. Table. 2 lists the results for the classification of viral and bacterial pneumonia after adding healthy samples in image-level prediction. Comparing with the above results, the accuracy has increased from 89.2% to 93.69% and all other indicators have improved significantly. Fig. 3 (b) shows the improved confusion matrix for binary classification task. Comparing the two

sub-figures we can see that the number of samples classified incorrectly has decreased to 7 samples. For the three-classification of viral, bacterial patients

Table 3. Comparison of Different Method for Three-classification task

Method	Accuracy	Precision	Recall	F1 score
DeCoVNet	0.897	0.882	0.850	0.861
AD3D-MIL	0.906	0.937	0.841	0.861
DRENet	0.942	0.945	0.946	0.945
JMFNet w/o Local	0.890	0.903	0.900	0.895
JMFNet w/o GAT	0.931	0.935	0.931	0.932
JMFNet(our method)	**0.955**	**0.956**	**0.958**	**0.957**

and healthy persons, keeping the above training process, we only need to add healthy person samples to the test set. The number of healthy CT sequences are 44 in the test set. Table. 3 shows the comparison results of different methods and our model has still achieved the best results. Fig. 4 shows the confusion matrix for three-classification task. For bacterial patients, there are four misdiagnosed cases, which are regarded as viral infection. Two viral patients were diagnosed with bacterial infection and one was identified as a healthy person.

4.3 Interpretability

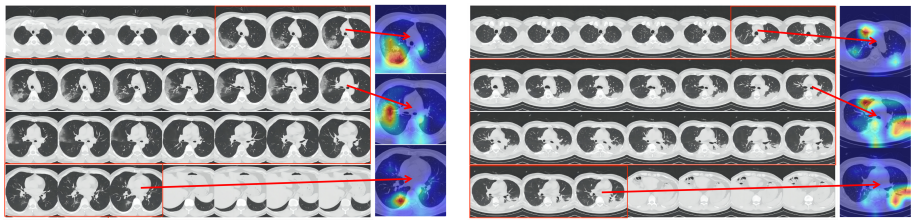

Fig. 5. Visualization of patients with pneumonia by different etiologies on CT images. The difference in CT appearance between viral and bacterial pneumonia is shown from left to right.

To provide explainable diagnostic basis for radiologists, we show the several important slices and their visual maps by Gradient-weighted Class Activation Mapping (Grad-CAM) [27] in Fig. 5. For viral and bacterial pneumonia, the location of the lesions are different. The lesions of viral pneumonia mainly appears in the subpleura, while those of bacterial pneumonia are mainly concentrated in the lung parenchyma [28]. From the figure we can see that the proposed model

has payed more attention to the lesion regions, which can clearly reflect the location information of the lesions. The visualization results are consistent with the clinical diagnosis basis, which further verifies the reliability of our method.

5 Conclusion

With the development of computer vision technology, artificial intelligence-assisted disease diagnosis performs excellent functions in clinical preliminary screening. In this study, we propose a joint multi-view feature network for automatic diagnosis of pneumonia based on chest CT sequences. We implemented the detection of focus regions and features aggregation by fusing CNN and graph attention module. Aims to explore the location relationship and dependency relations of local lesions, we add a Faster-RCNN branch on the backbone and construct graph attention network to extract the embeddings of lesions. The accuracy has improved by 0.65% comparing with the that without considering local features. The experiments demonstrate the feasibility and superiority of the proposed method.

References

1. N. P. Dueck et al. “Atypical Pneumonia: Definition, Causes, and Imaging Features”. In: Radiographics 41.3 (2021), p. 200131.
2. Min Lang et al. “Pulmonary Vascular Manifestations of COVID-19 Pneumonia”. In: Radiology Cardiothoracic Imaging 2.3 (2020), e200277.
3. F. Shi et al. “Review of Artificial Intelligence Techniques in Imaging Data Acquisition, Segmentation and Diagnosis for COVID-19”. In: IEEE Reviews in Biomedical Engineering PP.99 (), pp. 1–1.
4. M. Traub et al. “The use of chest computed tomography versus chest X-ray in patients with major blunt trauma.” In: Injury-international Journal of the Care of the Injured 38.1 (2007), pp. 43–47.
5. J. Lei et al. “CT Imaging of the 2019 Novel Coronavirus (2019-nCoV) Pneumonia”. In: Radiology 295.1 (2020), p. 18.
6. Xi Zhan et al. “Dandelion and focal crazy paving signs: the lung CT based predictors for evaluation of the severity of coronavirus disease”. In: Current Medical Research and Opinion ().
7. P. Parag and T. C. Hardcastle. “Interpretation of Emergency CT Scans of the Head in Trauma: Neurosurgeon vs Radiologist”. In: World Journal of Surgery: Official Journal of the Societe Internationale de Chirurgie, Collegium Internationale Chirurgiae Digestivae, and of the International Association of Endocrine Surgeons 46-6 (2022).
8. Supriya V. Mahadevkar et al. “A Review on Machine Learning Styles in Computer Vision—Techniques and Future Directions”. In: IEEE Access 10 (2022), pp. 107293–107329. doi: 10.1109/ACCESS.2022.3209825.
9. Vishan Kumar Gupta et al. “Prediction of COVID-19 confirmed, death, and cured cases in India using random forest model”. In: Big Data Mining and Analytics 4.2 (2021), pp. 116–123. doi: 10.26599/BDMA.2020.9020016.

10. C. Jin et al. “Development and Evaluation of an AI System for COVID- 19”. In: (2020).
11. A. Krizhevsky, I. Sutskever, and G. Hinton. “ImageNet Classification with Deep Convolutional Neural Networks”. In: Advances in neural information processing systems 25.2 (2012).
12. Safynaz Abdel-Fattah Sayed, Abeer Mohamed Elkorany, and Sabah Sayed Mohammad. “Applying Different Machine Learning Techniques for Prediction of COVID-19 Severity”. In: IEEE Access 9 (2021), pp. 135697–135707. doi: 10.1109/ACCESS.2021.3116067.
13. Shouliang Qi A B et al. “DR-MIL: Deep represented multiple instance learning distinguishes COVID-19 from community-acquired pneumonia in CT images”. In: Computer Methods and Programs in Biomedicine (2021).
14. K. He et al. “Deep Residual Learning for Image Recognition”. In: IEEE Conference on Computer Vision and Pattern Recognition. 2016.
15. Ying Song et al. “Deep Learning Enables Accurate Diagnosis of Novel Coronavirus (COVID-19) With CT Images”. In: IEEE/ACM Transactions on Computational Biology and Bioinformatics 18.6 (2021), pp. 2775–2780. doi: 10.1109/TCBB.2021.3065361.
16. T. N. Kipf and M. Welling. “Semi-Supervised Classification with Graph Convolutional Networks”. In: (2016).
17. X. Yu et al. “ResGNet-C: A graph convolutional neural network for detection of COVID-19”. In: Neurocomputing (2020).
18. Petar Velikovi et al. “Graph Attention Networks”. In: (2017).
19. H. Takebe. “Development of similar CT image retrieval technology based on lesion natures and their three-dimensional distribution”. In: (2017).
20. S. Ren et al. “Faster R-CNN: Towards Real-Time Object Detection with Region Proposal Networks”. In: IEEE Transactions on Pattern Analysis Machine Intelligence 39.6 (2017), pp. 1137–1149.
21. T. Y. Lin et al. “Feature Pyramid Networks for Object Detection”. In: 2017 IEEE Conference on Computer Vision and Pattern Recognition (CVPR). 2017.
22. K. Simonyan and A. Zisserman. “Very Deep Convolutional Networks for Large-Scale Image Recognition”. In: Computer Science (2014).
23. Christian Szegedy et al. “Going Deeper with Convolutions”. In: IEEE Computer Society (2014).
24. G. Huang et al. “Densely Connected Convolutional Networks”. In: IEEE Computer Society (2016).
25. Xinggang Wang et al. “A Weakly-Supervised Framework for COVID-19 Classification and Lesion Localization From Chest CT”. In: IEEE Transactions on Medical Imaging 39.8 (2020), pp. 2615–2625. doi: 10. 1109 / TMI.2020.2995965.
26. Zhongyi Han et al. “Accurate Screening of COVID-19 Using AttentionBased Deep 3D Multiple Instance Learning”. In: IEEE Transactions on Medical Imaging 39.8 (2020), pp. 2584–2594. doi: 10. 1109 / TMI. 2020. 2996256.
27. Ramprasaath R. Selvaraju et al. “Grad-CAM: Visual Explanations from Deep Networks via Gradient-Based Localization”. In: 2017 IEEE International Conference on Computer Vision (ICCV). 2017, pp. 618–626. doi: 10.1109/ICCV.2017.74.
28. N. Johansson, M. Kalin, and J. Hedlund. “Clinical impact of combined viral and bacterial infection in patients with community-acquired pneumonia.” In: Scandinavian Journal of Infectious Diseases 43.8 (2011), pp. 609– 615.